Finite-Time Backstepping of a Nonlinear System in Strict-Feedback Form: Proved by Bernoulli Inequality

ZHENGRU REN[1,2], BO ZHAO[3], AND DONG TRONG NGUYEN[2]
[1]Centre for Research-based Innovation of Marine Operations (SFI MOVE), NO-7491 Trondheim, Norway
[2]Department of Marine Technology, Norwegian University of Science and Technology (NTNU), NO-7491 Trondheim, Norway
[3]School of Automation, Harbin Engineering University, Harbin 150001, China

Corresponding author: Zhengru Ren (zhengru.ren@ntnu.no)

ABSTRACT In this paper, we propose a novel state-feedback backstepping control design approach for a single-input single-output (SISO) nonlinear system in strict-feedback form. Rational-exponent Lyapunov functions (ReLFs) are employed in the backstepping design, and the Bernoulli inequality is primarily adopted in the stability proof. Semiglobal practical finite-time stability, or global asymptotically stability, is guaranteed by a continuous control law using a commonly used recursive backstepping-like approach. Unlike the inductive design of typical finite-time backstepping controllers, the proposed method has the advantage of reduced design complexity. The virtual control laws are designed by directly canceling the nonlinear terms in the derivative of the specific Lyapunov functions. The terms with exponents are transformed into linear forms as their bases. The stability proof is simplified by applying several inequalities in the final proof, instead of in each step. Furthermore, the singularity problem no longer exists. The weakness of the concept of practical finite-time stability is discussed. The method can be applied to smoothly extend numerous design methodologies with asymptotic stability with a higher convergence rate near the equilibrium. Two numerical case studies are provided to present the performance of the proposed control.

INDEX TERMS Finite-time stability, rational-exponent Lyapunov function, backstepping, Lyapunov methods, Bernoulli inequality.

I. INTRODUCTION

It is known that asymptotic and exponential stabilities imply the system trajectory converges to the equilibrium as time approaches infinity resulting in a slow convergence rate near the equilibrium, i.e., $\lim_{t \to \infty} x(t, x_0) = 0$ where x_0 is the initial state. In practice, fast response and high-precision tracking performance may be preferred over asymptotic stability. Arising in time-optimal control, the finite-time control technique has a faster response and better disturbance-rejection ability, which ensures the convergence to the equilibrium in finite time, i.e., $\lim_{t \to T} x(t, x_0) = 0$ and $x(t, x_0) = 0$, for all $t \geq T$ where T is the settle time [1]. Compared with the typical backstepping approaches that grantee asymptotic stability, the finite-time stability

allows a system to converge to the origin even when more than one equilibrium exists. In addition, the finite-time stable system has higher robustness and disturbance-rejection capability.

Finite-time stability is a higher requirement than the asymptotic stability. Several Lyapunov stability theorems for global finite-time stabilizability are given in literature, i.e., $\dot{V} + \lambda_1 V^\gamma \leq 0$ [1], $\dot{V} + \lambda_1 V^\gamma + \lambda_2 V \leq 0$ [16], [24], $\dot{V} + \lambda_1 V^\gamma + \lambda_2 V^\kappa \leq 0$ [19], where V is the Lyapunov function, $\lambda_1, \lambda_2 > 0$, $0 < \gamma < 1$, and $\kappa > 1$ are coefficients. Moreover, a weaker statement is the practical finite-time stability. The tracking error converges to a region in the settle time. The corresponding Lyapunov stabilities are in the forms such that $\dot{V} + \lambda_1 V^\gamma \leq \rho$ [21], [28] and $\dot{V} + \lambda_1 V^\gamma + \lambda_2 V \leq \rho$ [23], where $\rho > 0$. Finite-time stability can be also extended to stochastic nonlinear systems [22] and switched nonlinear systems [5].

The associate editor coordinating the review of this manuscript and approving it for publication was Di He.

Backstepping is a Lyapunov-based recursive design procedure for strict-feedback systems [3], [6], [10]–[13], [15], [17], [20], [25], [27]. The main idea is to divide the entire system into several subsystems and to recursively design a global controller according to the former subsystem. The design complexity of the controllers based on finite-time stability is higher than those according to asymptotic stability. Compared with the asymptotic-stability design, the inductive step, sign function, and changing coefficients for different steps complicate the design procedures [1], [2], [7], [8]. Quadratic Lyapunov function candidates (LFCs) are normally selected. The sign function helps to overcome the singularity problem caused by the term $x_i^{1/r}$ when r is an even integer, but it may introduce the zero-crossing issue in the simulations. The power integrator technique is used to handle the sign function [5], [9], [18]. Hence, the cancellation-based design approach is difficult. Applying several inequalities in each step also enhances the complexity of the backstepping design.

There already exist a significant number of studies on adaptive backstepping design with a focus on semiglobal stability, such as robust adaptive control and neural adaptive control [3], [20], [25]. To overcome the system uncertainty and nonlinearity, the Lyapunov criteria with a final form $\dot{V} \leq -\lambda_1 V + \rho$ ensures the system error stays within a specific region as $t \to \infty$. The boundary is determined by the values of λ_1 and ρ. However, it is difficult to extend the research outcomes to be finite-time stable.

In this paper, we propose a simple and systematic approach to construct practical finite-time trajectory tracking control for the strict-feedback nonlinear system. Compared to the relevant existing results in the literature [23], the main contributions of this paper are summarized as follows.

- The proposed design is recursive based on cancellation, while the complex inductive design is required in the foregoing studies. The proposed virtual control laws are simpler with constant coefficients instead of step-varying coefficients.
- The complexity, caused by the different exponents, in the deduction is moved from the virtual control laws to the selection of LFCs. The inequalities are only necessary to be used in the final proof, rather than applying inequalities in the deduction in every step. Thus, the derivative complexity is significantly reduced.
- To the best of the authors' knowledge, the Bernoulli's inequality is primarily introduced to the finite-time stability proof, which converts the terms with exponents such that they are the same order of their bases.
- The coefficients λ_1 and λ_2 can be predefined before the design process. The control gains are selected accordingly.
- The proposed method is compatible with other well-known backstepping design methods, such as neural adaptive control and robust adaptive control. Hence, the existing adaptive backstepping methods on all sorts of system uncertainties and nonlinearities can

be extended to the problem of finite-time stabilization smoothly.

II. PROBLEM FORMULATION AND PRELIMINARIES

For the simplicity, system uncertainties and other complexities are disregarded hereafter. Without loss of generality, consider the following n-dimensional lower-triangular SISO strict-feedback nonlinear system

$$
\begin{aligned}
\dot{x}_i &= f_i(\bar{x}_i) + g_i(\bar{x}_i)x_{i+1}, \quad i = 1, \cdots, n-1, \\
\dot{x}_n &= f_n(\bar{x}_n) + g_n(\bar{x}_n)u, \\
y &= x_1,
\end{aligned} \tag{1}
$$

where $x_1, \cdots, x_n \in \mathbb{R}$ are the states, $\bar{x}_i = [x_1, x_2, \cdots, x_i]^\top \in \mathbb{R}^i, y \in \mathbb{R}$ is the system output, $u \in \mathbb{R}$ is the control signal, and functions $f_i, g_i : \mathbb{R}^i \mapsto \mathbb{R}$ are known. In addition, we denote $x = \bar{x}_n$ and $z = [z_1, \cdots, z_n]^\top \in \mathbb{R}^n$.

The control objective is to construct a control law u such that the output x_1 tracks the desired trajectory $x_{1d}(t)$ for any initial conditions in finite time. Quite commonly-used assumptions for backstepping-like design are made on system (1).

Assumption 1 [20]: The functions $f_1, \cdots, f_n$, $i = 1, \cdots, n$ are smooth. There exists a positive constant g_0 such that $0 < g_0 \leq g_i(\bar{x}_i)$ for all $t > t_0$. The desired trajectory is assumed to be sufficiently smooth, i.e., the reference signal $x_{1d}(t)$ and its derivatives up to the nth-order are known, bounded, and continuous.

Definition 1 [28]: The solution of a nonlinear system

$$
\dot{x} = f(x) \tag{2}
$$

is practical finite-time stable if for all $x(t_0) = x_0$, there exists $\varepsilon > 0$ and $T(\varepsilon, x_0) < \infty$ such that $\|x(t)\| < \varepsilon$ for all $t \geq t_0 + T$.

The statement of finite-time stability denotes finite-time convergence and Lyapunov stability.

Lemma 1 [23]: Consider the nonlinear system (2), the origin $x = 0$ is a finite-time-stable equilibrium if there exists a continuous positive definite function $V(x)$, real numbers $\lambda_1 > 0$, $\lambda_2 > 0$, $\gamma \in (0, 1)$, and $0 < \rho < \infty$ such that

$$
\dot{V}(x) \leq -\lambda_1 V^\gamma(x) - \lambda_2 V(x) + \rho. \tag{3}
$$

The residual set of the solution of system $\dot{x} = f(x)$ is given by

$$
\left\{ \lim_{t \to T} V(x) \leq \min \left\{ \frac{\rho}{(1-\theta_0)\lambda_2}, \left(\frac{\rho}{(1-\theta_0)\lambda_1} \right)^{\frac{1}{\gamma}} \right\} \right\}, \tag{4}
$$

where $\theta_0 \in (0, 1)$ and

$$
\begin{aligned}
T \leq \max\{ &t_0 + \frac{1}{\theta_0\lambda_2(1-\gamma)} \ln \frac{\theta_0\lambda_2 V^{1-\gamma}(t_0) + \lambda_1}{\lambda_1}, \\
&t_0 + \frac{1}{\lambda_2(1-\gamma)} \ln \frac{\lambda_2 V^{1-\gamma}(t_0) + \theta_0\lambda_1}{\theta_0\lambda_1} \}. \tag{5}
\end{aligned}
$$

Remark 1 The practical finite-time stability can be both proven by $\dot{V} \leq -\lambda_1 V^\gamma - \lambda_2 V + \rho$ and $\dot{V} \leq -\lambda_1 V^\gamma + \rho$.

The former one has a faster convergence rate in the region far away from the equilibrium [13].

Remark 2 The necessity and reasonability of Definition 1 will be discussed in Section IV. Though the concept is doubtable, the LFC (3) ensures a faster convergence near the equilibrium.

Lemma 2 (Bernoulli's Inequality [14]): For $0 \leq r \leq 1$ and real number $x \geq -1$, the following relation holds,

$$(1+x)^r \leq 1 + rx. \tag{6}$$

Remark 3 Bernoulli's inequality is very useful to transform the rational-exponent terms into forms with the same exponent as their bases. It is the first time that the Bernoulli's inequality is introduced to the finite-time stability proof. The inequality sign in the Bernoulli's inequality is determined by the selection of r. The inequality is feasible in a subset of the domain of a real number.

A rational-exponent Lyapunov function (ReLF) is constructed in a form

$$V(x) = \frac{1}{2}[(1+x^2)^r - 1], \quad r \in (0,1). \tag{7}$$

It is easy to find that $V(0) = 0$ and $V(x) > 0$ for all $x \in \mathbb{R}/0$. As $1 + x^2 \geq 1$, the derivative of V with respect to x, $dV/dx = rx(1+x^2)^{r-1}$, is constantly positive, indicating that $V(x)$ is strictly increasing. In addition, $\lim_{x \to \infty} V(x) = \infty$. Hence, the function $V(x)$ is radically unbounded and belongs to class $\mathcal{K}_\infty$.

Remark 4 According to (6), $V(x) \leq \frac{1}{2}rx^2$. From the figures, it can be concluded that the error between $V(x)$ and $\frac{1}{2}rx^2$ decrease as x tends to 0. When $r = 1$, (7) is a quadratic LFC.

Lemma 3 [9]: For any $x_i \in \mathbb{R}$, $i = 1, \cdots, n$ and a real number $r \in (0,1]$, the following inequality holds

$$\left(\sum_{i=1}^n |x_i|\right)^r \leq \sum_{i=1}^n |x_i|^r \leq n^{1-r}\left(\sum_{i=1}^n |x_i|\right)^r. \tag{8}$$

III. CONTROL LAW DESIGN

First, the errors are defined as $z_1 := x_1 - x_{1d}$, $z_i := x_i - \alpha_{i-1}$, $i = 2 \cdots, n$, where α_i is the virtual control law in the ith step which will be designed later.

Step 1: Consider the nonlinear system (1), the error dynamics are given by

$$\dot{z}_1 = f_1(\bar{x}_1) + g_1(\bar{x}_1)x_2 - \dot{x}_{1d}. \tag{9}$$

Choose the LFC as $V_1(z_1) = \frac{1}{2}[(1+z_1^2)^{r_1} - 1]$, where $r_1 \in (0,1)$ is a design parameter. Recalling $z_2 = x_2 - \alpha_1$ and substituting (9), the time derivative of V_1 becomes

$$\dot{V}_1 = r_1(1+z_1^2)^{r_1-1}z_1[f_1 + g_1(\alpha_1 + z_2) - \dot{x}_{1d}]. \tag{10}$$

Establish the virtual controller as

$$\alpha_1 = \frac{1}{g_1}[-f_1 + \dot{x}_{1d} - \frac{c_1}{r_1}(1+z_1^2)^{1-r_1}z_1], \tag{11}$$

where $c_1 > 0$ is the control gain to be discussed later.

Substituting (11) into (10) yields

$$\dot{V}_1 = -c_1 z_1^2 + r_1 g_1(1+z_1^2)^{r_1-1}z_1 z_2. \tag{12}$$

Step i ($2 \leq i \leq n-1$): Let the LFC for the ith step be

$$V_i = V_{i-1} + \frac{1}{2}[(1+z_i^2)^{r_i} - 1], \tag{13}$$

where $r_i \in (0,1)$ is a design parameter.

Differentiating V_i yields

$$\begin{aligned}
\dot{V}_i &= \dot{V}_{i-1} + r_i(1+z_i^2)^{r_i}z_i\dot{z}_i \\
&= -\sum_{j=1}^{i-1} c_j z_j^2 + r_{i-1}g_{i-1}(1+z_{i-1}^2)^{r_{i-1}-1}z_{i-1}z_i \\
&\quad + r_i(1+z_i^2)^{r_i-1}z_i[f_i + g_i(z_{i+1} + \alpha_i) - \dot{\alpha}_{i-1}].
\end{aligned} \tag{14}$$

The virtual controller is adopted as

$$\begin{aligned}
\alpha_i = \frac{1}{g_i}\Big[&-f_i + \dot{\alpha}_{i-1} - \frac{1}{r_i}(1+z_i^2)^{1-r_i} \\
&\times \big(r_{i-1}g_{i-1}(1+z_{i-1}^2)^{r_{i-1}-1}z_{i-1} + c_i z_i\big)\Big],
\end{aligned} \tag{15}$$

where $c_i > 0$ is the control gain. Substituting (15) into (14) yields

$$\dot{V}_i = -\sum_{j=1}^i c_j z_j^2 + r_i g_i(1+z_i^2)^{r_i-1}z_i z_{i+1}. \tag{16}$$

Step n: Choose the LFC as follows

$$V_n = V_{n-1} + \frac{1}{2}[(1+z_n^2)^{r_n} - 1], \tag{17}$$

where $r_n \in (0,1)$ is a design parameter.

The time derivative of V_n is

$$\begin{aligned}
\dot{V}_n &= \dot{V}_{n-1} + r_n(1+z_n^2)^{r_n-1}z_n\dot{z}_n \\
&= -\sum_{i=1}^{n-1} c_i z_i^2 + r_{n-1}g_{n-1}(1+z_{n-1}^2)^{r_{n-1}-1}z_{n-1}z_n \\
&\quad + r_n(1+z_n^2)^{r_n-1}z_n(f_n + g_n u - \dot{\alpha}_{n-1}).
\end{aligned} \tag{18}$$

The controller is chosen as

$$\begin{aligned}
u = \frac{1}{g_n}\Big[&-f_n + \dot{\alpha}_{n-1} - \frac{1}{r_n}(1+z_n^2)^{1-r_n} \\
&\times \big(r_{n-1}g_{n-1}(1+z_{n-1}^2)^{r_{n-1}-1}z_{n-1} + c_n z_n\big)\Big],
\end{aligned} \tag{19}$$

where $c_n > 0$ is the control gain.

Substituting (19) into (18) yields,

$$\dot{V}_n \leq -\sum_{i=1}^n c_i z_i^2. \tag{20}$$

Theorem 1: For the nonlinear system (1) under assumption 1, the tracking error z_1 converges into a disc region with radius

$$\min\left\{\sqrt{[2\frac{\rho}{(1-\theta_0)\lambda_2}+1]^{\frac{1}{r_1}} - 1}, \right.$$

$$\left. \sqrt{\left[2\left(\frac{\rho}{(1-\theta_0)\lambda_1}\right)^{\frac{1}{\gamma}}+1\right]^{\frac{1}{r_1}} - 1}\right\}$$

in finite time if the virtual control laws and the control input are chosen as (11), (15), and (19) with $\gamma \in (0, 1)$, $\lambda_1 > 0$, $\lambda_2 > 0$, $r_i \in (0, 1)$, and the control gains satisfying

$$c_i \geq (\frac{\lambda_1 \gamma}{2\gamma} + \frac{\lambda_2}{2})r_i. \qquad (21)$$

The closed-loop system is bounded in finite time.

Proof: Substituting (11), (15), and (19), the resulting closed-loop error dynamics are

$$\dot{z}_1 = -\frac{c_1}{r_1}(1 + z_1^2)^{1-r_1} z_1 + g_1 z_2, \qquad (22a)$$

$$\dot{z}_i = -\frac{r_{i-1}g_{i-1}(1 + z_i^2)^{1-r_i}}{r_i(1 + z_{i-1}^2)^{1-r_{i-1}}} z_{i-1} \qquad (22b)$$
$$\quad -\frac{c_i}{r_i}(1 + z_i^2)^{1-r_i}z_i + g_i z_{i+1} \quad i = 2, \cdots, n-1,$$

$$\dot{z}_n = -\frac{r_{n-1}g_{n-1}(1 + z_n^2)^{1-r_n}}{r_n(1 + z_{n-1}^2)^{1-r_{n-1}}} z_{n-1} \qquad (22c)$$
$$\quad -\frac{c_n}{r_n}(1 + z_n^2)^{1-r_n}z_n.$$

For the LFC $V(z) = V_n$, by Lemma 2, (20) becomes

$$\dot{V}(z) = -\sum_{i=1}^{n} \varepsilon_i[\frac{c_i}{\varepsilon_i}z_i^2] \leq \sum_{i=1}^{n} \left[\varepsilon_i - \varepsilon_i(1 + z_i^2)^{c_1/\varepsilon_i} \right], \qquad (23)$$

where $0 < \varepsilon_i < \frac{c_i}{r_i}$ is an arbitrary real number. We will later show that the selection of ε_i does not influence the results.

Let $\lambda_1 > 0$ and $\gamma \in (0, 1)$,

$$\lambda_1 V^{\gamma}(z) = \frac{\lambda_1}{2\gamma} \left(\sum_{i=1}^{n} [(1 + z_i^2)^{r_i} - 1] \right)^{\gamma}. \qquad (24)$$

To cancel the proper fractional exponent γ in (24), applying lemmas 3 and 2 yields

$$\lambda_1 V^{\gamma}(z) \leq \frac{\lambda_1}{2\gamma} \sum_{i=1}^{n} \left[(1 + z_i^2)^{r_i} - 1 \right]^{\gamma}$$
$$\leq \frac{\lambda_1}{2\gamma} \sum_{i=1}^{n} \left[\gamma \left((1 + z_i^2)^{r_i} - 2 \right) + 1 \right]$$
$$= \frac{\lambda_1}{2\gamma} \sum_{i=1}^{n} \gamma(1 + z_i^2)^{r_i} + \frac{\lambda_1 n}{2\gamma}(1 - 2\gamma). \qquad (25)$$

Substituting (23) and (25) into $\dot{V}(z) + \lambda_1 V^{\gamma}(z) + \lambda_2 V(z)$ yields

$$\dot{V}(z) + \lambda_1 V(z)^{\gamma} + \lambda_2 V(z) \leq \sum_{i=1}^{n} \Big[\varepsilon_i - \varepsilon_i(1 + z_i^2)^{c_i/\varepsilon_i}$$
$$+ (\frac{\lambda_1 \gamma}{2\gamma} + \frac{\lambda_2}{2})(1 + z_i^2)^{r_i} + \frac{\lambda_1}{2\gamma}(1 - 2\gamma) - \frac{\lambda_2}{2} \Big]. \qquad (26)$$

Define $\chi := z_i^2 \geq 0$ and $h(\chi) := \varepsilon_i - \varepsilon_i(1 + \chi)^{c_i/\varepsilon_i} + (\frac{\lambda_1 \gamma}{2\gamma} + \frac{\lambda_2}{2})(1 + \chi)^{r_i} + \frac{\lambda_1}{2\gamma}(1 - 2\gamma) - \frac{\lambda_2}{2}$.

The derivative of $h(\chi)$ with respect to χ is given by

$$\frac{dh(\chi)}{d\chi} = -c_i(1 + \chi)^{c_i/\varepsilon_i - 1} + (\frac{\lambda_1 \gamma}{2\gamma} + \frac{\lambda_2}{2})r_i(1 + \chi)^{r_i - 1}. \qquad (27)$$

To find the extrema of $h(\chi)$, let $\frac{dh(\chi)}{d\chi} = 0$. Then, the only extremum is found at $\chi_e = \left[\frac{r_i}{c_i}(\frac{\lambda_1 \gamma}{2\gamma} + \frac{\lambda_2}{2}) \right]^{\frac{\varepsilon_i}{c_i - \varepsilon_i r_i}} - 1$. In addition, $h(0) = \frac{\lambda_1}{2\gamma}(1 - \gamma)$ and $h'(0) = -c_i + (\frac{\lambda_1 \gamma}{2\gamma} + \frac{\lambda_2}{2})r_i$.
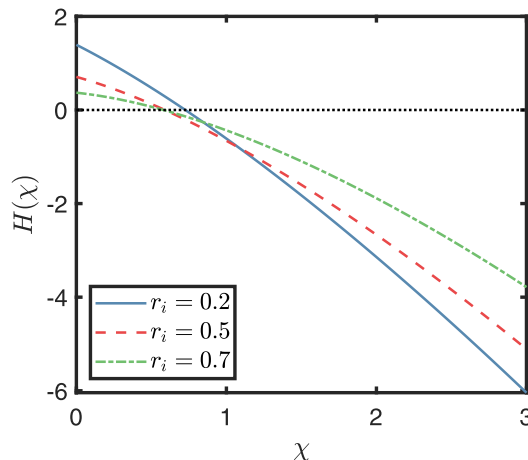

FIGURE 1. Function $H(\chi)$ with respect to χ ($\lambda_1 = 2$, $\lambda_2 = 3$, $c_i = 2$, $\varepsilon_i = 1.5$, $r_i \in \{0.2, 0.5, 0.7\}$, and $\gamma = r_i$).

If the gains c_i are selected such that (21) holds, $h'(0) \leq 0$ and $\frac{r_i}{c_i}(\frac{\lambda_1 \gamma}{2\gamma} + \frac{\lambda_2}{2}) \in (0, 1]$. Hence, the extrema can be found in the domain $\chi_e \in (-1, 0]$ with arbitrarily selected $0 < r_i < 1$ and $0 < \varepsilon_i < \frac{c_i}{r_i}$. Since $h'(0) \leq 0$, the function $h(\chi)$ is monotonically decreasing when $\chi \geq 0$, shown in Figure 1. Applying the above results to (26), we find the maximum for $\dot{V}(z) + \lambda_1 V(z)^{\gamma} + \lambda_2 V(z)$ as

$$\dot{V}(0) + \lambda_1 V(z)^{\gamma}(0) + \lambda_2 V(0) = \frac{\lambda_1 n}{2\gamma}(1 - \gamma) =: \rho. \qquad (28)$$

Therefore, $\dot{V}(z) + \lambda_1 V(z)^{\gamma} + \lambda_2 V(z) \leq \rho$ is proven and the practical finite-time stability of the system (22) is proven according to Lemma 1. The value of ρ is influenced by λ_1, λ_2, c_i, r_i, and γ. ☐

Remark 5: The most remarkable advantage of the proposed method is that the design procedure follows the classic cancellation-based recursive approach. Inductive steps are no longer needed. The design procedure is greatly simplified.

Remark 6: The selection of ε_i in (23) does not influence the value of ρ.

Remark 7: The control gains c_i are designed according to the preset λ_1, λ_2, and γ.

Remark 8: In the virtual control laws (11) and (15) and final control law (19), the terms $(1 + z_i^2)^{1-r_i}$ amplify the controller and contribute to a more aggressive convergence when z_i is far away from the equilibrium point in (22).

Remark 9: In the deduction, the singularity is no longer an issue, since the bases for the exponent $r_i - 1$ are always in a form of $1 + z_i^2$, which is larger than 1.

Remark 10: The convergence rate is determined by the design parameters r_i and control gains c_i, $i = 1, \cdots, n$. Smaller r_i and higher c_i enhance the convergence rate.

Remark 11: When $\lambda_2 = 0$, the semiglobal practical finite-time stability is still ensured, i.e., $\dot{V} \leq \lambda_1 V + \rho$.

The boundary is explicit, i.e., the disc region is $V(t \geq t_0 + T) \leq \left(\frac{\rho}{\lambda_1}\right)^{1/\gamma}$ and the radius is

$$z_i = \sqrt{[2(\frac{\rho}{\lambda_1})^{1/\gamma} + 1]^{1/r_1} - 1}. \tag{29}$$

Easy to find that the convergence rate is faster and the disc region is smaller with increasing λ_2, if λ_1 remains the same value. Hence, the disc region that the tracking error converges to by the proposed controller is smaller than that in (29).

IV. DISCUSSION ON PRACTICAL FINITE-TIME STABILITY

Let us first review the concept of practical finite-time stability in Definition 1. Actually, any asymptotic stability with LFC

$$\dot{V} \leq -\lambda_1 V + \rho, \tag{30}$$

with $\lambda_1 > 0$ and $\rho > 0$ satisfies the practical finite-time stability. Times $\exp(-\lambda_1 t)$ to both sides of (30), yields $\dot{V} \exp(-\lambda_1 t) + \lambda_1 V \exp(\lambda_1 t) \leq \rho \exp(\lambda_1 t)$. Integrate both side yields, $\frac{d}{dt} V \exp(\lambda_1 t) \leq \frac{\rho}{\lambda_1} \frac{d}{dt} \exp(\lambda_1 t)$. Define $\delta := \rho/\lambda_1$ and integrating along $[0, t]$ yields $0 \leq V(t) \leq \delta + (V(0) - \delta) \exp(-\lambda_1 t)$ [26]. If the boundary is selected as $\bar{V} \geq \delta$, then for any $t \geq -\frac{1}{\lambda_1} \ln[\frac{\bar{V}-\delta}{V(0)-\delta}]$, $V(t) \leq \bar{V}$, i.e., the error goes into the a region disk after a center time. "Practical" finite-time stability can also be achieved by the LFC (30). By (20), easy to prove that the error dynamics (22) is global asymptotically stable. Hence, the practical finite-time stability can be achieved by global asymptotically stability with sufficiently large control gains. More details will be given in a future publication.

Besides the proposed ReLF, we have to point out that the semiglobal practical finite-time stability is also satisfied by the quadratic LFC, which can be proved by interested readers.

Admittedly, the concept of practical finite-time stability is doubtable. However, the key point of the present paper is the employment of the Bernoulli inequality in the stability proof. The additional LFC component, V^γ, enhances the convergence rate near the origin. Hence, it is possible to consider the resulting close-loop system is also global asymptotically stable.

V. SIMULATION RESULTS

The performance of the proposed algorithm is verified via two case studies.

A. CASE STUDY 1: 2-ORDER INTEGRATOR CHAIN

A simplest 2-order integrator chain is presented as an example, i.e.,

$$\dot{x}_1 = x_2, \tag{31a}$$
$$\dot{x}_2 = u. \tag{31b}$$

The resulting error dynamics are given by

$$\dot{z}_1 = -\frac{c_1}{r_1}(1 + z_1^2)^{1-r_1} z_1 + g_1 z_2, \tag{32a}$$

$$\dot{z}_2 = -\frac{r_1 g_1 (1 + z_2^2)^{1-r_2}}{r_2 (1 + z_1^2)^{1-r_1}} z_1 - \frac{c_2}{r_2}(1 + z_2^2)^{1-r_2} z_2. \tag{32b}$$

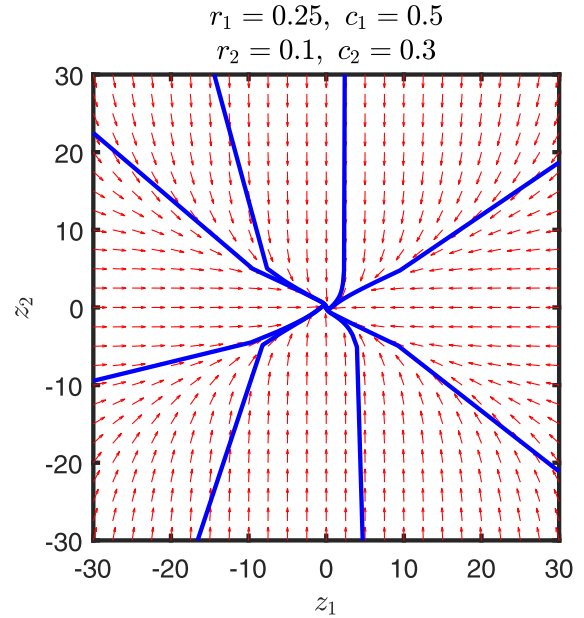The phase portraits of the three groups of design coefficients are presented in figs. 2–3, where a red arrow shows

FIGURE 2. Phase portrait when $r_1 = 0.25$, $c_1 = 0.5$, $r_2 = 0.1$, $c_2 = 0.3$.
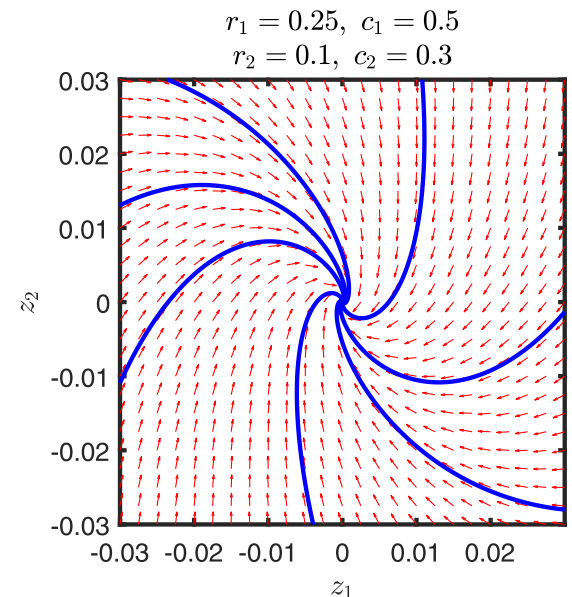
FIGURE 3. Phase portrait when $r_1 = 0.25$, $c_1 = 0.5$, $r_2 = 0.1$, $c_2 = 0.3$, Zoomed in.

the direction of flow from that point, and each blue line indicates a system's trajectory. From the phase portraits, we can summarize that the closed-loop system is stable and the convergence rate for the ith dimension can be tuned by the corresponding r_i and c_i. In addition, ideal sliding surfaces are not found.

B. CASE STUDY 2: ELECTROMECHANICAL SYSTEM

The dynamics of a single-link robot manipulator and a motor rotor [4], [23] is given by

$$M\ddot{q} + B\dot{q} + N\sin(q) = I, \tag{33a}$$
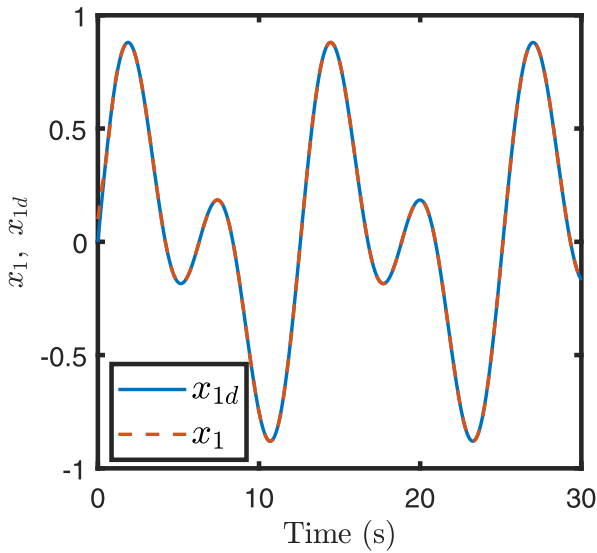$$L\dot{I} = V_e - RI - K_B\dot{q}, \tag{33b}$$

FIGURE 4. Tracking trajectory x_1 and x_{1d} under the proposed controller.
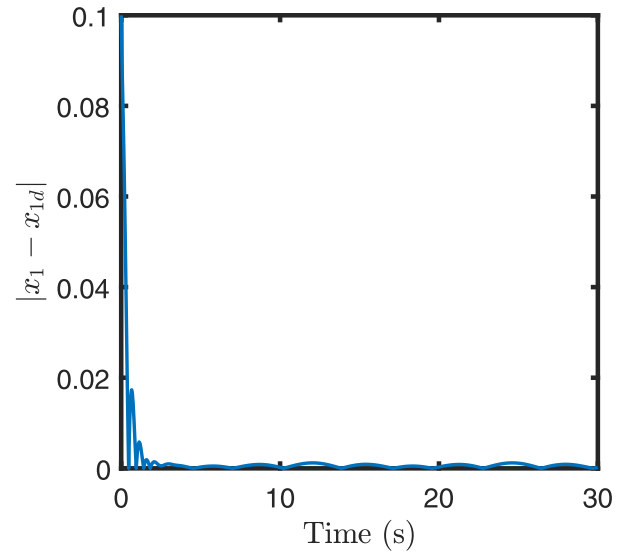

FIGURE 6. Tracking error $|x_1 - x_{1d}|$.
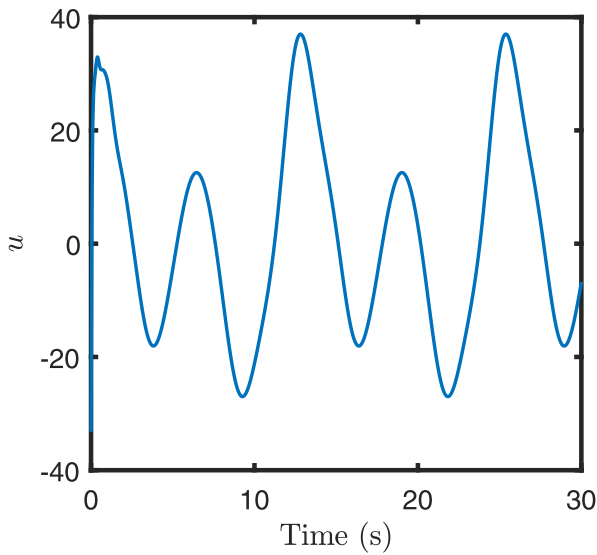

FIGURE 5. Control input u under the proposed controller.
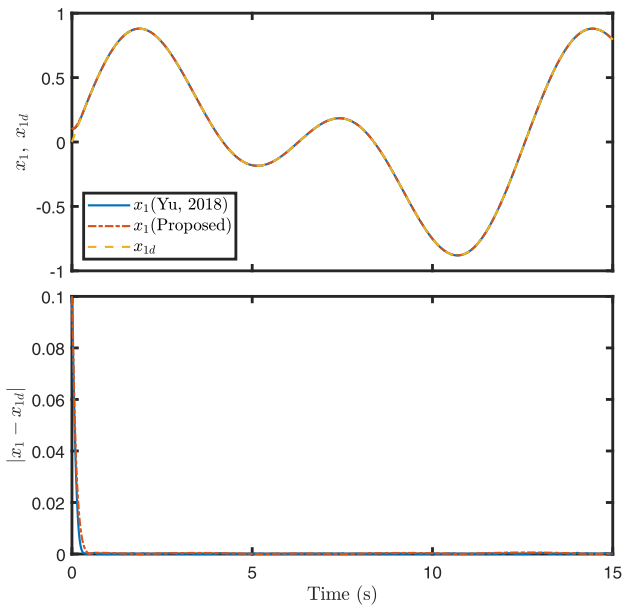

FIGURE 7. Comparison between the proposed method and [23] (upper: trajectories of x_1 and x_{1d}, lower: tracking error $|x_1 - x_{1d}|$).

where q is the angular motor position, I is the motor armature current,

$$M = \frac{1}{K_\tau}\left(J + \frac{mL_0^2}{3} + M_0L_0^2 + \frac{2M_0R_0^2}{5}\right),$$

$$N = \frac{1}{K_\tau}\left(\frac{mL_0G}{2} + M_0L_0g\right) \quad B = \frac{B_0}{K_\tau},$$

J is the rotor inertia, m is the link mass, M_0 is the load mass, L_0 is the link length, R_0 is the radius of the load, G is the gravity coefficient, B_0 is the coefficient of viscous friction at the joint, K_τ is the coefficient that characterizes the electromechanical conversion of armature current to torque, L is the armature inductance, R is the armature resistance, K_B is the back EMF coefficient, and V_e is the input control voltage.

Define the states and input as $x_1 = q$, $x_2 = \dot{q}$, $x_3 = I$, and $u = V_e$, (33) is rewritten as

$$\dot{x}_1 = x_2, \tag{34a}$$

$$\dot{x}_2 = -\frac{N}{M}\sin(x_1) - \frac{B}{M}x_2 + \frac{1}{M}x_3, \tag{34b}$$

$$\dot{x}_3 = -\frac{K_B}{L} - \frac{R}{L}x_3 + \frac{1}{L}u, \tag{34c}$$

$$y = x_1, \tag{34d}$$

where $G = 9.81$, $J = 1.625e - 3$, $m = 0.506$, $R_0 = 0.023$, $M_0 = 0.434$, $L_0 = 0.305$, $B_0 = 16.25e{-3}$, $K_B = K_\tau = 0.9$, $L = 15$, and $R = 5.0$. The desired trajectory is $x_{1d}(t) = 0.5\sin(t) + 0.5\sin(0.5t)$. The initial condition is $[x_1, x_2, x_3]^\top = [0.1, 0.5, 0.5]^\top$; The design parameters are selected as $r_1 = 0.05$, $c_1 = 0.5$, $r_2 = 0.1$, $c_2 = 0.3$, $r_3 = 0.5$, and $c_3 = 0.6$.

The simulation results are presented in figs. 4–6. The system output quickly converges to the desired trajectory. After the settle time, the error remains within a boundary. The control input is smooth and stays in a reasonable range. Since sign functions do not exist in the controller, the zero-crossing issue is released and resulting in shorter computation time.

The results of a comparison study to [23] is shown in Figure 7. The control gains and parameter are tuned accordingly. Compared to [23], the computation time is much shorter. This is because the proposed method does not requires the error-compensation signals and the additional states introduced by the command filter. The fast eigenfrequencies in the command filter dynamics need very small time step. Moreover, the oscillations in the control input is smaller.

VI. CONCLUSION

The paper presents a novel state-feedback recursive practical finite-time backstepping design method for a class of SISO nonlinear systems in strict-feedback form using an innovative rational-exponent Lyapunov function. The proposed controller simplifies the practical finite-time backstepping design. The exponents in the LFCs and the controller gains are still subject to some constraints, and the control design procedures are based on cancellation. Furthermore, Bernoulli's inequality is introduced to prove the finite-time stability for the first time, which reduces the deduction complexity by removing the exponents. In addition, the simulation results illustrate the performance of the controller.

Though the concept of practical finite-time stability is doubtable, the proposed control design provides another design method with proved stability which enhances the convergence rate near the origin by employing a stricter LFC.

REFERENCES

[1] S. P. Bhat and D. S. Bernstein, "Finite-time stability of continuous autonomous systems," *SIAM J. Control Optim.*, vol. 38, no. 3, pp. 751–766, Jan. 2000.

[2] C.-C. Chen and Z.-Y. Sun, "A unified approach to finite-time stabilization of high-order nonlinear systems with an asymmetric output constraint," *Automatica*, vol. 111, Jan. 2020, Art. no. 108581.

[3] M. Chen, S. Sam Ge, and B. How, "Robust adaptive neural network control for a class of uncertain MIMO nonlinear systems with input nonlinearities," *IEEE Trans. Neural Netw.*, vol. 21, no. 5, pp. 796–812, May 2010.

[4] D. M. Dawson, J. J. Carroll, and M. Schneider, "Integrator backstepping control of a brush DC motor turning a robotic load," *IEEE Trans. Control Syst. Technol.*, vol. 2, no. 3, pp. 233–244, Sep. 1994.

[5] J. Fu, R. Ma, and T. Chai, "Global finite-time stabilization of a class of switched nonlinear systems with the powers of positive odd rational numbers," *Automatica*, vol. 54, pp. 360–373, Apr. 2015.

[6] S. S. Ge, F. Hong, and T. H. Lee, "Robust adaptive control of nonlinear systems with unknown time delays," *Automatica*, vol. 41, no. 7, pp. 1181–1190, Jul. 2005.

[7] Y. Hong, "Finite-time stabilization and stabilizability of a class of controllable systems," *Syst. Control Lett.*, vol. 46, no. 4, pp. 231–236, Jul. 2002.

[8] Y. Hong, J. Huang, and Y. Xu, "On an output feedback finite-time stabilization problem," *IEEE Trans. Autom. Control*, vol. 46, no. 2, pp. 305–309, Feb. 2001.

[9] X. Huang, W. Lin, and B. Yang, "Global finite-time stabilization of a class of uncertain nonlinear systems," *Automatica*, vol. 41, no. 5, pp. 881–888, May 2005.

[10] I. Kanellakopoulos, P. V. Kokotovic, and A. S. Morse, "Systematic design of adaptive controllers for feedback linearizable systems," *IEEE Trans. Autom. Control*, vol. 36, no. 11, pp. 1241–1253, Nov. 1991.

[11] P. V. Kokotovic, "The joy of feedback: Nonlinear and adaptive," *IEEE Control Syst. Mag.*, vol. 12, no. 3, pp. 7–17, Jun. 1992.

[12] Y. Li, S. Tong, Y. Liu, and T. Li, "Adaptive fuzzy robust output feedback control of nonlinear systems with unknown dead zones based on a small-gain approach," *IEEE Trans. Fuzzy Syst.*, vol. 22, no. 1, pp. 164–176, Feb. 2014.

[13] Y. Liu, X. Liu, Y. Jing, and Z. Zhang, "Semi-globally practical finite-time stability for uncertain nonlinear systems based on dynamic surface control," *Int. J. Control*, vol. 2019, pp. 1–10, Apr. 2019.

[14] D. S. Mitrinovic, J. Pecaric, and A. M. Fink, *Classical and New Inequalities in Analysis*, vol. 61. Delft, The Netherlands: Springer, 2013.

[15] Z. Ren, Z. Jiang, Z. Gao, and R. Skjetne, "Active tugger line force control for single blade installation," *Wind Energy*, vol. 21, no. 12, pp. 1344–1358, Dec. 2018.

[16] Y. Shen and X. Xia, "Semi-global finite-time observers for nonlinear systems," *Automatica*, vol. 44, no. 12, pp. 3152–3156, Dec. 2008.

[17] K. Sun, L. Liu, J. Qiu, and G. Feng, "Fuzzy adaptive finite-time fault-tolerant control for strict-feedback nonlinear systems," *IEEE Trans. Fuzzy Syst.*, to be published.

[18] Z.-Y. Sun, L.-R. Xue, and K. Zhang, "A new approach to finite-time adaptive stabilization of high-order uncertain nonlinear system," *Automatica*, vol. 58, pp. 60–66, Aug. 2015.

[19] Z.-Y. Sun, M.-M. Yun, and T. Li, "A new approach to fast global finite-time stabilization of high-order nonlinear system," *Automatica*, vol. 81, pp. 455–463, Jul. 2017.

[20] K. P. Tee, S. S. Ge, and E. H. Tay, "Barrier Lyapunov functions for the control of output-constrained nonlinear systems," *Automatica*, vol. 45, no. 4, pp. 918–927, Apr. 2009.

[21] F. Wang, B. Chen, C. Lin, J. Zhang, and X. Meng, "Adaptive neural network finite-time output feedback control of quantized nonlinear systems," *IEEE Trans. Cybern.*, vol. 48, no. 6, pp. 1839–1848, Jun. 2017.

[22] J. Yin, S. Khoo, Z. Man, and X. Yu, "Finite-time stability and instability of stochastic nonlinear systems," *Automatica*, vol. 47, no. 12, pp. 2671–2677, Dec. 2011.

[23] J. Yu, P. Shi, and L. Zhao, "Finite-time command filtered backstepping control for a class of nonlinear systems," *Automatica*, vol. 92, pp. 173–180, Jun. 2018.

[24] S. Yu, X. Yu, B. Shirinzadeh, and Z. Man, "Continuous finite-time control for robotic manipulators with terminal sliding mode," *Automatica*, vol. 41, no. 11, pp. 1957–1964, Nov. 2005.

[25] T. Zhang, "Adaptive neural network control for strict-feedback nonlinear systems using backstepping design," *Automatica*, vol. 36, no. 12, pp. 1835–1846, Dec. 2000.

[26] T. P. Zhang and S. S. Ge, "Adaptive dynamic surface control of nonlinear systems with unknown dead zone in pure feedback form," *Automatica*, vol. 44, no. 7, pp. 1895–1903, Jul. 2008.

[27] H. Zhao, J. Zheng, W. Deng, and Y. Song, "Semi-supervised broad learning system based on manifold regularization and broad network," *IEEE Trans. Circuits Syst. I: Reg. Papers*, vol. 67, no. 3, pp. 983–994, Mar. 2020.

[28] Z. Zhu, Y. Xia, and M. Fu, "Attitude stabilization of rigid spacecraft with finite-time convergence," *Int. J. Robust Nonlinear Control*, vol. 21, no. 6, pp. 686–702, Apr. 2011.

ZHENGRU REN received the B.Eng. degree in naval architecture and offshore engineering from the Dalian University of Technology, Dalian, China, in 2012, and the M.Sc. and Ph.D. degrees in marine technology from the Norwegian University of Science and Technology (NTNU), Trondheim, Norway, in 2015 and 2019, respectively. From April to August 2019, he was a Researcher with the Department of Ocean Operations and Civil Engineering, NTNU. He is currently a Postdoctoral Research Fellow with the Centre for Research-based Innovation on Marine Operations (SFI MOVE), Department of Marine Technology, NTNU. His research interests are within nonlinear control theory, sensor fusion, offshore wind energy, marine installation, and dynamic positioning system.

BO ZHAO received the bachelor's degree in automation and the master's degree in navigation, guidance, and control from the Beijing University of Aeronautics and Astronautics (BUAA), in 2006 and 2009, respectively, and the Ph.D. degree in marine cybernetics from the Norwegian University of Science and Technology, in 2015. From 2013 to 2018, he served as a Senior Marine System Advisor for Global Maritime, where he developed hardware-in-the-loop testing for dynamic positioning systems. He is currently an Associate Professor with Harbin Engineering University. His research interests include applying advanced control and artificial intelligence in the control of vessel, underwater robotics, and other marine systems.

DONG TRONG NGUYEN received the B.S. degree (Hons.) in civil engineering from the Ho Chi Minh City University of Technology (HCMUT), Ho Chi Minh City, Vietnam, in 2001, and the Ph.D. degree in civil engineering from the Department of Civil Engineering, National University of Singapore (NUS), Singapore, in 2006. He was a Postdoctoral Researcher at the Centre of Ships and Ocean Structures (CeSOS), NTNU, from 2006 to 2008. Since 2008, he has been working with Marine Cybernetics AS and DNV GL involving hardware-in-the-loop testing of marine and offshore control systems, digital twins, and digitalization of the maritime industry and ocean assets. He is currently an Adjunct Associate Professor with the Department of Marine Technology, NTNU. His research interests are supervisory switching control and nonlinear control with applications to marine control systems, digital twin, and digitalization.

• • •